

Nonlinear Geometric Fuzzy Logic Control for DC Motor Drive Systems

F. XEPAPAS, A. KALETSANOS, S. XEPAPAS, S. MANIAS
 Department of Electrical and Computer Engineering
 National Technical University of Athens
 Iroon Polytechneioy 9, T.K. 15772 & 15700
 ATHENS GREECE

Abstract: - This paper presents the Geometric fuzzy logic controller, properly modified in order to be used in DC motor drive systems. The controller with Geometric fuzzy logic technique is a nonlinear robust controller very promising for high performance solutions. The required components for the implementation of the Geometric fuzzy logic controller are similar with the well-known PI controller. The advantage of the Geometric fuzzy logic controller is the better tracking response of the control system with minimum dependency on the motor parameters. In this paper the Geometric fuzzy logic controller is compared with a PI controller for controlling the speed of a DC motor and the advantages are distinct.

Key-Words: - Geometrical Control, Sliding Mode, Switching line, DC Motor Fuzzy Logic.

1 Introduction

In this paper a DC Motor drive system is analyzed with a constant field excitation. For such a DC Motor, the rotor (armature) that is rotating with shaft speed (ω), is producing back-EMF voltage $E=E(\omega)$. Therefore, in order to keep that speed it must feed armature with terminal voltage u . The value of u is counteraction to the E . That results to the armature current value i as showing in Fig.1.

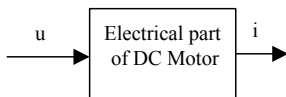


Fig.1: Electrical part of the DC Motor

The relationships between u and i are given by the following well known expressions:

$$u - E = iR + L \frac{di}{dt} \quad \text{or} \quad (1)$$

$$u - E = (R + sL)i \quad (2)$$

where: R = armature Resistance
 L = armature Inductance

The mechanical part of the DC Motor model is showing in Fig.2.

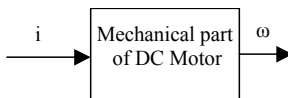


Fig.2: Mechanical part of a DC Motor

The relationships between i and ω are given by the following expressions:

$$T - T_L = J \frac{d\omega}{dt} \quad \text{or} \quad (3)$$

$$K_T i - T_L = J \frac{d\omega}{dt} \quad (4)$$

where:

K_T = electromechanical Torque constant

T_L = Load Torque

J = Inertia of the motor and load mass

2 Theme Formulation

The conventional control structure of a DC Motor drive system for speed control is showing in Fig.3.

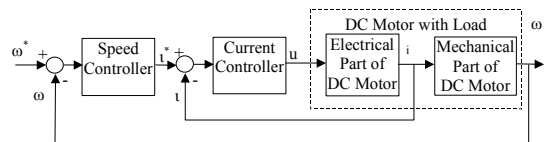


Fig.3: Conventional control structure of a DC Motor drive system

In order to control the mechanical part output variable (ω), a speed controller is needed. Also, in order to control the electrical part output (armature current), a current controller is needed. According to eqn(4) armature current i changes linearly with the motor speed

$$\text{acceleration } \frac{d\omega}{dt}.$$

3 Solution

Instead of using two separated controllers for ω and i , as shown in Fig. 3, this paper proposes one controller that will control the speed (ω) and change of speed. Let $\omega^*(t)$ be the speed reference, $\omega(t)$ the real speed value, so the speed error $e = \omega^* - \omega$ indicates the speed tracking error. Fig.4 shows the proposed control block diagram.

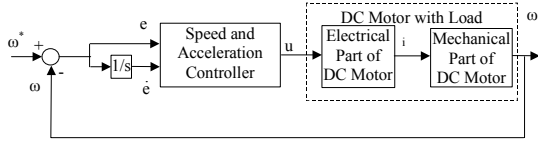


Fig.4: The proposed control block diagram

The DC motor model in state space is given by:

$$\dot{x} = A(t) \cdot x + B(t) \cdot u + f(t) \quad (5)$$

where:

$$x = [x_1, x_2]^T = [e, \dot{e}]^T$$

$$A = \begin{bmatrix} 0 & 1 \\ -\alpha_1 & -\alpha_2 \end{bmatrix}, \quad B = \begin{bmatrix} 0 \\ \frac{K_T}{J \cdot L} \end{bmatrix}$$

$$\text{where } \alpha_1 = K_T \cdot \frac{K_e}{J \cdot L}, \quad \alpha_2 = \frac{R}{L}$$

The nonlinear model, expressed by eqn(5), has control input variable u for minimizing the speed error ($e \rightarrow 0$) and the speed error acceleration ($\dot{e} \rightarrow 0$). In order to control the above nonlinear system, the Geometric control technique is used. Geometric control means that the control input value u changes discontinuously when the trajectories of state eqn(5) cross a switching boundary at the phase plane (e, \dot{e}). Since eqn(5) is a second order system, the switching boundary function must be of a first-order.

Let define the switching line as:

$$s = ce + \dot{e} \quad (6)$$

with c being a positive constant and the voltage source for the DC motor as:

$$u = M \text{sgn}(s) \quad (7)$$

According to eqn(6) and eqn(7) the system trajectories have reflective behavior. In this case, switching action $u = M \text{sgn}(s)$, immediately redirects the system motion back without allowing the boundary to be crossed. So after a trajectory crosses line $s = ce + \dot{e} = 0$, with control action $u = M \text{sgn}(s)$, the movement cannot leave the switching line. The system motion is now:

$$s = ce + \dot{e} = 0 \quad (8)$$

and is directed to the equilibrium point $O(e=0, \dot{e}=0)$, sliding on the switching line, with a rate of convergence determined by the value of c . The system motion in state space is shown in Fig. 5.

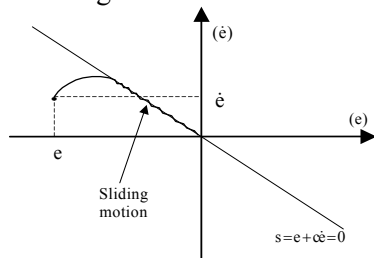


Fig.5: System motion in state space

With the proposed method it is capable to control e and \dot{e} with stable, fast and robust way. The result of the controller using $u = M \text{sgn}(s)$, is ideal. In reality eqn(5) can be constructed as follows:

$$u = M \cdot \text{sat} \begin{cases} M \cdot \text{sgn}(s) & \text{for } |s| > \epsilon \\ \frac{M}{\epsilon} \cdot s & \text{for } |s| \leq \epsilon \end{cases} \quad (9)$$

The above function characteristic is shown in Fig. 6.

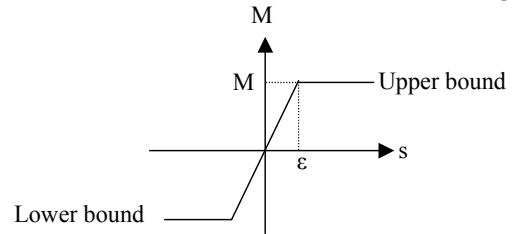


Fig.6: Characteristic of eqn(9)

The ideal case is the limit of $u = M \text{sgn}(s)$ with $\epsilon \rightarrow 0$.

$$\text{So } u = \lim_{\epsilon \rightarrow 0} M \cdot \text{sgn}(s) \quad (10)$$

The implementation of eqn(10) is difficult in real time mode. In order to solve the above problem this paper presents a modified control block diagram as shown in Fig. 7.

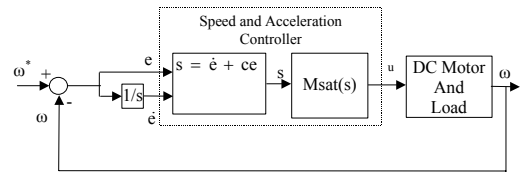


Fig.7: Proposed modified DC motor control block diagram

This method provides a linear transfer characteristic with lower and upper bounds (Fig. 6). In this paper, a new method introduced, in which the transfer characteristic is not necessarily a straight line between these bounds, but a curve that can be adjusted to reflect given performance requirements. This transfer characteristic is shown in Fig. 8.

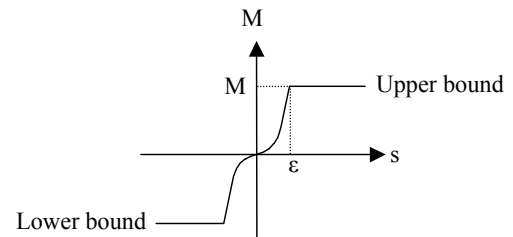


Fig.8: Characteristic of eqn(11)

The expression of u is now given by:

$$u = M \cdot \text{sat} \begin{cases} M \cdot \text{sgn}(s) & \text{for } |s| > \epsilon \\ \frac{M_{\text{fuzzy}}(|Sp|, d)}{\epsilon} \cdot s & \text{for } |s| \leq \epsilon \end{cases} \quad (11)$$

where: $M_{fuzzy}(|Sp|,d)$ is not a constant gain but a variable gain selected from a fuzzy rule-based controller. Assuming that our system is in point $P(e',\dot{e}')$ the values $|Sp|$ and d are defining as follows:

$$|Sp| = \frac{|s|}{\sqrt{1+c^2}}$$

is the distance between the switching line $s=ce+\dot{e}=0$ and point P while d is the distance (parallel to switching line) from point P to the point O . (Fig. 9).

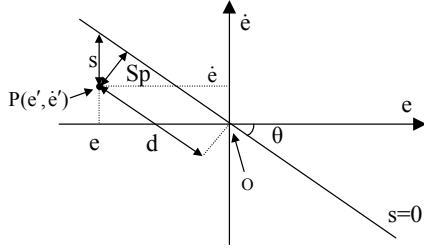


Fig.9: Schematic presentation of the new variables Sp and d .

An important parameter of the system is the constant c . If the controlled system (eqn.5) is a second-order system then c determines the slop of the switching line $s=0$. The parameter c plays the role of a break frequency. Parameter c has to be designed in such a way that unmodeled frequencies v_{un} are filtered out. Let v_{unmin} be a lower bound of v_{un} . Then c has to be designed such that $c \ll v_{unmin}$. Assuming that unmodeled frequencies occur above the eigenfrequency ω of the system (eqn.5) it is easy to choose $c \leq \omega$. The eigenfrequency of (eqn.5), obtaining from the homogeneous equation:

$$\ddot{e} + \alpha_2 \dot{e} + \alpha_1 e = 0 \quad (12)$$

Which can be rewritten as:

$$\ddot{e} + 2\zeta\omega \dot{e} + \omega^2 e = 0 \quad (13)$$

Hence, eigenfrequency obtaining from:

$$\omega = \sqrt{\alpha_1} \quad (14)$$

4 Fuzzy Controller

4.1 Structure of fuzzy rule-based controller

The computational structure of the fuzzy rule-based controller is shown in Fig. 10.

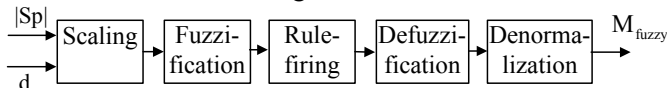


Fig.10: Block diagram of a rule-based fuzzy controller

There are five such computational steps constituting the fuzzy rule-based controller. These are the following:

1. Input scaling (normalization).
2. Fuzzification of controller-input variables.
3. Inference (rule firing).
4. Defuzzification of controller-output variables.
5. Output scaling (denormalization).

4.2 The membership function distribution

The values $|Sp|$ and d are used as inputs to the fuzzy controller. The value of gain M_{fuzzy} is the output of the controller. The two input variables are divided into their fuzzy segments. The numbers of fuzzy segments are chosen to have maximum control with minimum number of rules. The grade of member distribution of input variables into their fuzzy segments is shown in Fig. 11.

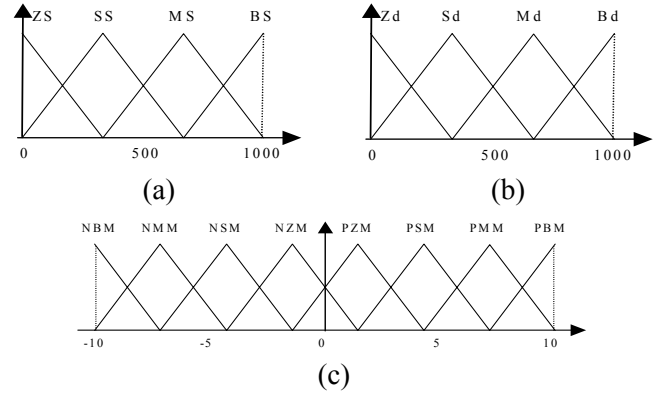


Fig.11: Membership functions distribution

- (a) input $|Sp|$
- (b) input d
- (c) output u

4.3 Input/output variables range

Working with variations of input variables an adaptation of real variables to fuzzy kernel has to be done to code the whole range within a constant range. The variation of input variable $|Sp|$ is coded within the range $[0, 1000]$ by multiplying by 2 and the variation of input variable d is coded within the range $[0, 1000]$ by dividing by 5. For the variation of the output variable M_{fuzzy} defined the range $[-10, 10]$ as shown in Fig. 11(c).

4.4 Definition of linguistic variables and fuzzy rules

Each control rule, can be described using the state variables $|Sp|$ and d and the control variable M_{fuzzy} . The i^{th} rule R_i can be written as:

$$R_i: \text{if } |Sp| \text{ is } A_i \text{ and } d \text{ is } B_i \text{ then } M_{fuzzy} \text{ is } N_i \quad (15)$$

where: A_i, B_i and N_i presents the linguistic variables as follows:

- | | | |
|---------|-----|------------------|
| A_i : | ZS: | (zero $ Sp $) |
| | SS: | (small $ Sp $) |
| | MS: | (medium $ Sp $) |
| | BS: | (big $ Sp $) |
| B_i : | Zd | (zero d) |
| | Sd | (small d) |
| | Md | (medium d) |
| | Bd | (big d) |

- N_i: NBM (negative big M_{fuzzy})
- NMM (negative medium M_{fuzzy})
- NSM (negative small M_{fuzzy})
- NZM (negative zero M_{fuzzy})
- PZM (positive zero M_{fuzzy})
- PSM (positive small M_{fuzzy})
- PMM (positive medium M_{fuzzy})
- PBM (positive big M_{fuzzy})

The control rules are formulated using the diagram of the transformation of the values e and \dot{e} to |Sp| and d (Fig. 9). There are sixteen rules, which are given in table1.

NBM	NBM	NBM	NBM	Bd
NMM	NBM	NBM	NBM	Md
NSM	NMM	NBM	NBM	Sd
NZM	NSM	NMM	NBM	Zd
ZS	NS	MS	BS	Sp \ d

Table.1 Control rules of the fuzzy controller

4.5 Fuzzy inference

The inference method used is basic and simple and is developed from the minimum operation rule as a fuzzy implementation function. The membership function of A, B and N are given by μ_A , μ_B and μ_N respectively. The firing strength of ith rule α_i can be expressed as:

$$\alpha_i = \min(\mu_{A_i}(|Sp|), \mu_{B_i}(d)) \quad (16)$$

By fuzzy reasoning using Mamdani's minimum operation rule as a fuzzy implication function, the ith rule leads to the control decision:

$$\mu_{N_i}(M_{fuzzy}) = \min(\alpha_i, \mu_{N_i}(M_{fuzzy})) \quad (17)$$

Thus the membership function μ_N of the output M_{fuzzy} is pointwise given by:

$$\mu_N(M_{fuzzy}) = \max_{i=1}^{16} (\mu_{N_i}(M_{fuzzy})) \quad (18)$$

Since the output is crisp, the centroid method is used for defuzzification. By this method, the crisp value of fuzzy output calculated by the following equation:

$$M'_{fuzzy} = \frac{\int M_{fuzzy} \cdot \mu(M_{fuzzy})}{\int \mu(M_{fuzzy}) \cdot dM_{fuzzy}} \quad (19)$$

5 Simulation

5.1 Simulation Setup

Simulation of the Geometrical Fuzzy Logic controller was carried out to verify the behavior of the controller. The program that was used for the simulation is the Simulink of Matlab. Fig. 12 shows the Simulink close loop block diagram of a speed controlled DC motor drive system.

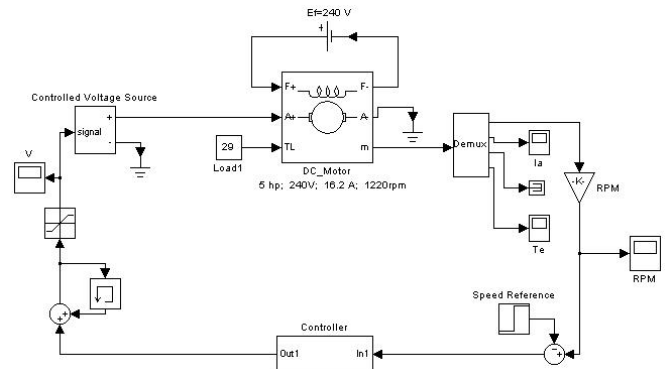


Fig.12: Simulink close loop block diagram for the DC motor speed control

Fig.13 shows the Simulink block diagram of the controller that utilizes the Geometric fuzzy logic technique.

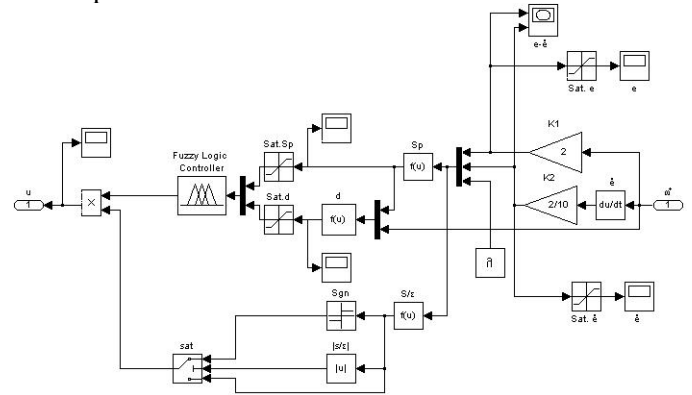


Fig.13: Controller based on Geometric fuzzy logic technique

In order to check the speed tracking error, the speed reference value changes at t=0.6sec from 1000RPM to 500RPM. The characteristics of the DC motor that is used for the simulation are the following:

- Induced EMF Eo=230.3 V
- Pe=5.0 HP
- Nominal torque Te=29.2 N.m
- Armature resistance Ra=0,6 ohms
- Armature inductance La=0,012 H
- Field resistance Rf=240 ohms
- Field inductance Lf=120 H
- Field-armature inductance Laf 1,8 H
- Total inertia J=1Kg.m²
- Viscous friction coefficient Bm=0 N.m.s
- Coulomb friction torque Tf=0 N.m
- Initial speed=0 rad/s.

5.2 Simulation Results

Fig. 14-17 show the operation of the DC motor with a controller based on the Geometric fuzzy logic technique. Moreover, Fig. 18-20 show the operation of the DC motor with a conventional controller (PI controller).

Simulation results with controller with Geometric fuzzy logic technique ($c=1, \epsilon=10$).

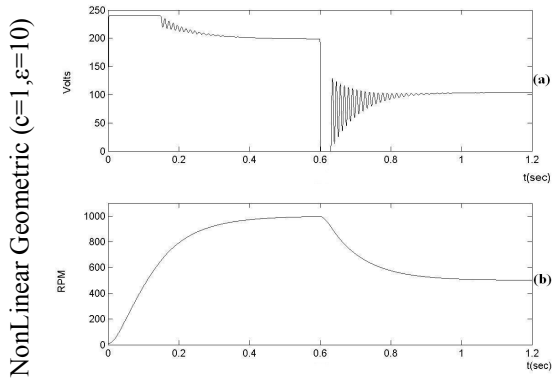


Fig. 14: (a) Voltage of the Armature, (b) Motor speed

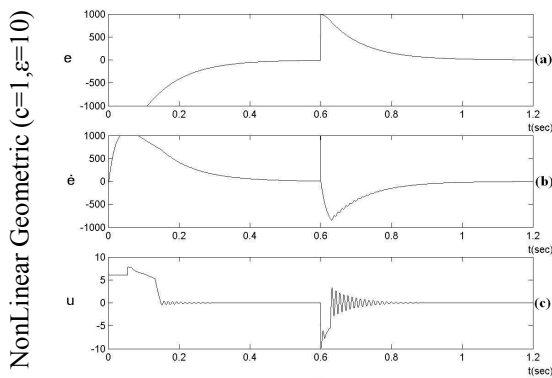


Fig. 15: (a) input error e , (b) change of error \dot{e} , (c) output u

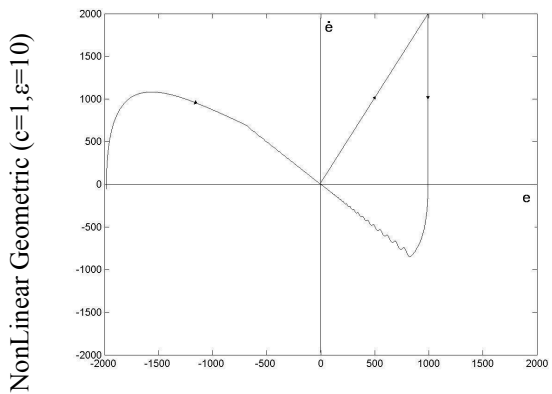


Fig. 16: Tracking

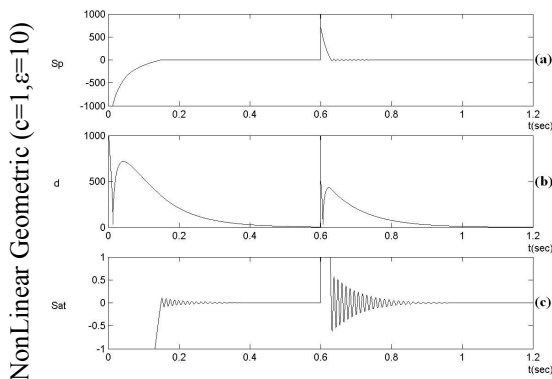


Fig. 17: Variables (a) S_p , (b) d , (c) sat

Simulation results with conventional PI controller.

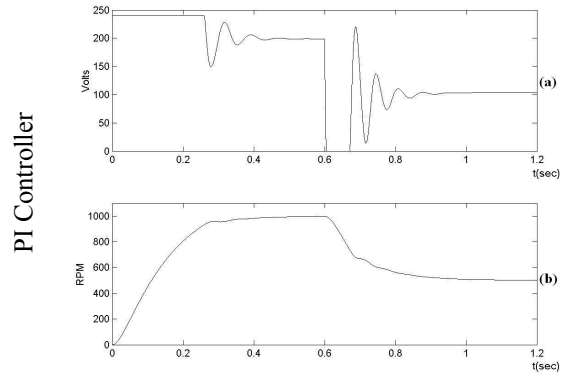


Fig. 18: (a) Voltage of the Armature, (b) Motor speed

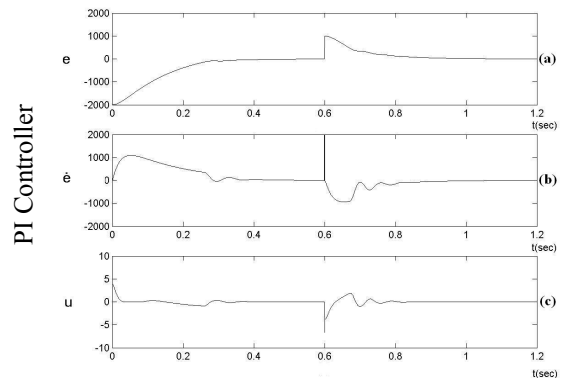


Fig. 19: (a) input error e , (b) change of error \dot{e} , (c) output u

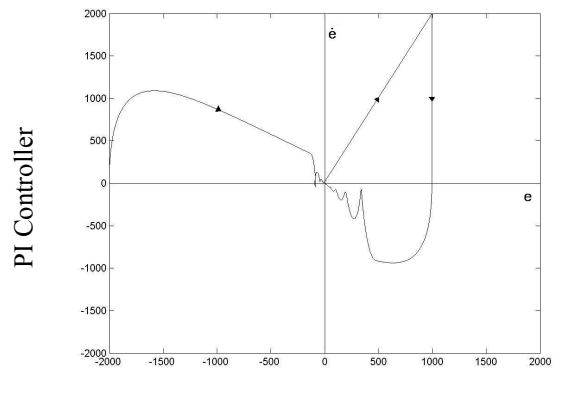


Fig. 20: Tracking

As it can be seen from Fig. 16 and Fig. 20 the minimization of the error and the derivative of the error of the speed is smoother with the Geometric fuzzy logic controller than with the conventional PI controller. With the Geometric fuzzy logic controller it can be achieved absolute control of the error and derivative of the error leading them to a desired point O. Fig. 21-24 shows the operation of the DC motor with a controller based on the Geometric fuzzy logic technique with $c=1.5$, instead of $c=1$ as it is in Fig. 14-17.

Simulation results with controller based on the Geometric fuzzy logic technique ($c=1.5, \epsilon=10$).

6 Conclusion

In this paper a Nonlinear Geometric Fuzzy Logic Controller for DC machines was presented. From the simulation results can be concluded that the proposed controller has better performance when is compared to the conventional PI controller. Although the input of the Geometrical Fuzzy logic controller is only the error of the speed, the response is better because it takes the advantage of the derivative of the speed error (acceleration).

References:

- [1] Rainer Palm, Dimiter Driankov, Hans Hellendoorn. *Model Based Fuzzy Control*, Springer, 1997.
- [2] John Yen, Reza Langary, Lotfi A. Zadeh. *Industrial Applications of Fuzzy Logic and Intelligent Systems*, IEEE Press, 1995
- [3] Mohammad Jamshidi, Nader Vadiee, Timothy J. Ross. *Fuzzy Logic and Control*, PTR Prentice Hall, 1993.
- [4] Witold Pedrycz, forward by Lotfi A. Zadeh. *Fuzzy Sets Engineering*, CRC Press, 1995
- [5] Witold Pedrycz, *Fuzzy Control and Fuzzy Systems*, Research Studies Press LTD, 1993.
- [6] Theoharis I. *Fuzzy Systems*, Aristoteleio University of Thessalonika Press, 1999.
- [7] Tzafestas Spyros. *Intelligent Automatic Control*, National Technical University of Athens, 1995.
- [8] V. Utkin, J. Gulder, J. Shi, *Sliding Mode Control in Electromechanical Systems*, Ed Taylor & Francis, 1999.
- [10] J.J. Slotine W.Li, *Applied Nonlinear Control*, Ed. Prentice Hall, 1991.
- [11] Vadim I. Utkin, *Sliding Mode Control Design Principles and Applications to Electric Drives*, IEEE Transactions On Industry Applications, vol.40, No.1, February 1993.

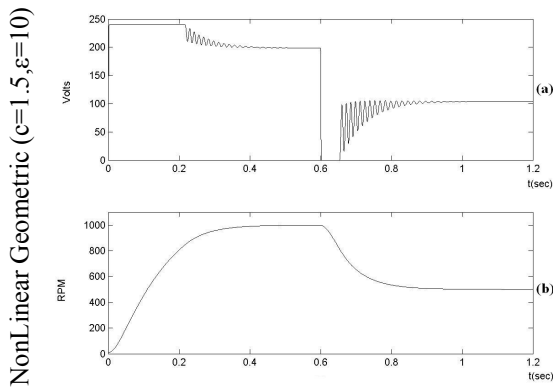


Fig 21: (a) Voltage of the Armature, (b) Motor speed

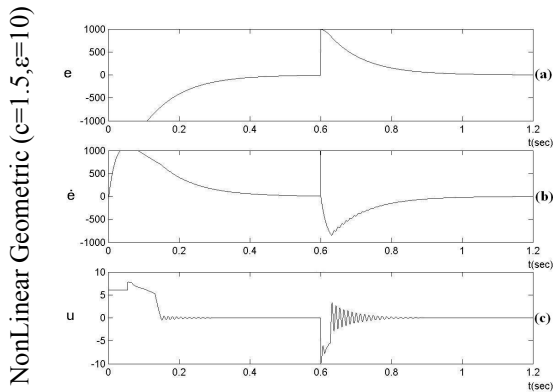


Fig.22: (a) input error e , (b) change of error \dot{e} , (c) output u

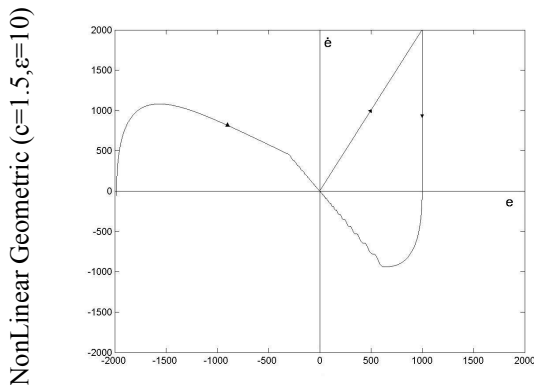


Fig.23: Tracking

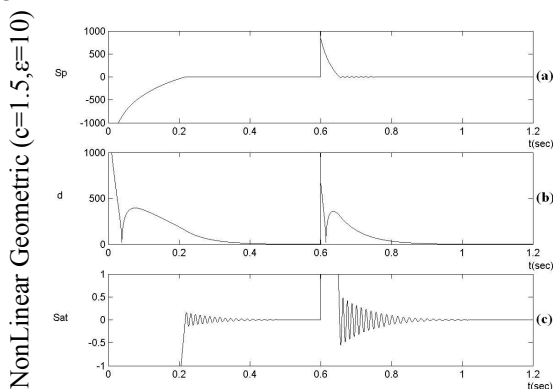


Fig.24: Variables (a) Sp , (b) d , (c) sat